Supplementary Information

Cyclic Topology Enhancing Structural Ordering and Stability of Comb-Shaped Polypeptoid Thin Films against Melt-Induced Dewetting

Naisheng Jiang,[1, 2 *] Jianxia Chen,[2] Tianyi Yu,[1] Albert Chao,[1] Liying Kang,[2] Ying Wu,[2] Kangmin Niu,[2] Ruipeng Li,[3] Masafumi Fukuto,[3] and Donghui Zhang[1 *]

[1.]Department of Chemistry and Macromolecular Studies Group, Louisiana State University, Baton Rouge, Louisiana 70803, United States

[2.]School of Materials Science and Engineering, University of Science and Technology Beijing, Beijing 100083, China

[3.]National Synchrotron Light Source II, Brookhaven National Laboratory, Upton, New York 11973, United States

Corresponding to: dhzhang@lsu.edu and naishengjiang@ustb.edu.cn

Experimental Section

General Considerations. Deuterated dichloromethane (99.8 atom % D) was purchased from Cambridge Isotope Laboratories. All other chemicals were purchased from Sigma Aldrich and used as received unless otherwise noted. All solvents used in polymerization were purified by passing through alumina columns under argon. ^{1}H NMR spectra were obtained using a Bruker AV-400 Nanobay spectrometer at 298 K. Chemical shifts (δ) given in parts per million (ppm) were referenced to protio impurities of deuterated solvents (CD_2Cl_2). MALDI-TOF mass spectra were collected using a Bruker UltrafleXtreme tandem time-of-flight (TOF) mass spectrometer. The instrument was calibrated with Peptide Calibration Standard II consisting of standard peptides Angiotensin I, Angiotensin II, Substance P, Bombesin, ACTH clip 1-17, ACTH clip 18-39, and Somatoratin 28 (Bruker Daltonics, Billerica, MA) prior to experiment. A saturated methanol solution of α-cyano-4-hydroxycinnamic acid was used as matrix. Samples were prepared by mixing a CH_2Cl_2 solution of polymers (10 mg/mL) with the matrix at 1:1 volume ratio, which were then deposited onto a 384-well ground-steel sample plate using a pipette and dried in air. Experiments were conducted in positive reflector mode. The data analysis was performed with FlexAnalysis software.

Polymer Synthesis. *N*-decylglycine derived *N*-carboxyanhydride (De-NCA) monomer was synthesized via the established procedure.[1, 2] Linear or cyclic poly(*N*-decylglycine)s (*l*/*c*-PNDG) were synthesized by a reported procedure involving the ring-opening polymerization of De-NCA monomer using either benzyl amine or *N*-heterocyclic carbene (NHC) initiators (Scheme S1).[3] The initial monomer to initiator ratio ($[M]_0$:$[I]_0$) was set to 50:1 and initial monomer concentration ($[M]_0$) is 0.4 M. All polymerizations were conducted in THF at 70 °C under nitrogen inside a glovebox for 48 h to reach a full conversion. The polymers were purified by precipitation in hexanes, a poor solvent for PNDG, then isolated and dried under vacuum prior to further analysis. The number-average degrees of polymerization (DP_n) and molecular weights (M_n) of *l*/*c*-PNDGs were determined by end-group analysis using ^{1}H NMR spectroscopy (Figure S1 - S2). The molecular weight distributions and polydispersity indices of the polymers were determined by MALDI-TOF MS analysis (Figure S3). The detailed molecular parameters of the *l*/*c*-PNDG polymer samples are summarized in Table S1.

Sample Preparation. Raw Si (100) wafers (purchased from University Wafer Inc.) were pre-

cleaned using a hot piranha solution (*i.e.*, a mixture of H_2SO_4 and H_2O_2, *caution: a* piranha solution *is highly corrosive upon contact with skin or eyes and is an explosion hazard when mixed with organic chemicals/materials; Extreme care should be taken when handing it*) for 30 min, and were subsequently rinsed with deionized water thoroughly. Such cleaning process gives a very hydrophilic surface due to the presence of a thin native oxide (SiO_x) layer. To create a hydrophobic surface, the piranha solution-cleaned Si wafers were further immersed in an aqueous solution of hydrogen fluoride (HF) for 30 s to remove the SiO_x layer, known as the HF-treated Si substrate. Since the *l*/*c*-PNDGs are hydrophobic in nature, it is expected that the HF-treated Si has a stronger interaction with PNDG than the native oxide Si. The static contact angle measurements (Figure S4) revealed that *l*-PNDG and *c*-PNDG have identical surface tension, and the interfacial energy between *l*/*c*-PNDGs and the HF-treated Si substrate is estimated to be $\gamma_{PNDG\text{-}HSi} = 10.7$ mJ/m^2, while the interfacial energy between the *l*/*c*-PNDGs and the native oxide Si substrate is estimated to be $\gamma_{PNDG\text{-}SiOxSi} = 14.9$ mJ/m^2. Hence, the HF-treated Si has a stronger affinity with *l*/*c*-PNDGs than the native oxide Si, which is attributed to the presence of long alkyl side chains of *l*/*c*-PNDGs. A series of *l*/*c*-PNDG thin films with different film thicknesses were prepared by spin coating *l*/*c*-PNDG/THF solutions onto the HF-treated Si with a rotational speed of 2500 rpm. The thicknesses of the spin-cast *l*/*c*-PNDG thin films were measured by X-ray reflectivity. The samples were annealed at temperatures at 200 °C far above the bulk melting temperatures of the polypeptoids ($T_m \approx 174$ ºC for *l*-PNDG and $T_m \approx 169$ ºC for *c*-PNDG)[3] for a prolonged period (15 h) under vacuum and subsequently cooled to room temperature (~ 22 °C) at a rate of approximately 150 °C/min prior to further characterization. We denote the HF-treated Si substrate as "Si substrate" in the main text and Supplementary Information.

To investigate the adsorbed polymer structure at the substrate interface, a top-down solvent leaching method, *a.k.a.* the Guiselin's approach,[4] was applied to the annealed *l*/*c*-PNDG films. Briefly, the *l*-PNDG and *c*-PNDG films that were pre-annealed at 200 °C for 15 h under vacuum were solvent leached in baths of fresh chloroform (a good solvent for both *l*/*c*-PNDGs) at 50 °C repeatedly until the resultant film thickness remained constant (typically a total of 4 cycles with 5 min per cycle). The change of thickness among each cycle was monitored by using a multi-wavelength spectroscopic ellipsometer (SE-VE ellipsometer, Wuhan Eoptics Technology Co. Ltd., China). All the final residual layers after chloroform leaching were then dried at 200 °C overnight under vacuum before further

characterization by XRR, GIWAXD and AFM.

Studies of Adsorption Kinetics of *l*/*c*-PNDGs on Si Substrate. The 48 nm-thick as-cast films on Si were first thermally annealed at 200 °C under vacuum for different annealing times and then solvent leached in baths of fresh chloroform at 50 °C repeatedly until the resultant film thickness remained constant (typically a total of 4 cycles with 5 min per cycle). The thicknesses of the *l*-PNDG and *c*-PNDG adsorbed layers as a function of annealing time was measured by a multi-wavelength spectroscopic ellipsometer (SE-VE ellipsometer, Wuhan Eoptics Technology Co. Ltd., China). The thicknesses of the adsorbed layers were determined by fitting the psi (ψ) and delta (δ) parameters as a function of wavelength using the Cauchy dispersion model.[5]

X-Ray Reflectivity (XRR). X-ray reflectivity experiments were performed using a synchrotron radiation source at the Complex Materials Scattering (CMS/11-BM) beamline at the National Synchrotron Light Source II (NSLS-II, Brookhaven National Laboratory). The X-ray energy was set as 13.5 keV (which is equivalent to a wavelength of λ = 0.0918 nm) by a multilayer monochromator with the energy resolution of 0.7%. The x-ray reflection was collected by using a photon-counting area detector (Dectris Pilatus 800k) placed 371 mm from the sample. The reflectivity intensity was collected by region of interests (ROIs) defined with the increase of incident angle. Additional XRR experiments were also performed using a laboratory source with a Bruker D8 Advance X-ray reflectometer employing Cu *K*α radiation with λ = 0.154 nm. Under specular reflection, the wavevector transfer, q_z, in the perpendicular direction to the film surface is given by $q_z = 4\pi\sin\theta/\lambda$, where θ is the incident angle. The XRR data was fit by using a standard multilayer fitting routine for a dispersion value (δ in the X-ray refractive index) in conjunction with a Fourier transformation (FT) method, a powerful tool to obtain detailed structures for low X-ray contrast polymer multilayers.[6] Note that δ is proportional to the electron density (ρ_e) by $\delta = \lambda^2\rho_e r_0/2\pi$, where r_0 is the classical electron radius.

Model Fitting of XRR Data. Based on the theoretical molecular dimensions of polypeptoid with a *cis*-amide conformation,[7] the ρ_e and the thickness values of the *cis*-amide middle layer are 0.42 $e\cdot$Å^{-3} and 4.4 Å, respectively, while the ρ_e and the thickness values of a single *n*-decyl layer are 0.30 $e\cdot$Å^{-3} and 9.85 Å, respectively (Figure 8). However, reasonable fits to the data cannot be achieved by strictly rely on the theoretical molecular dimensions of PNDG along *c*-axis. Rather, the best-fits to the data can be achieved by lowering the electron density and increase the thicknesses of the inner *n*-decyl

layers. To limit the number of free parameters during the fitting routing, ρ_e and thickness values of the outer *n*-decyl layer at the free surface and the middle *cis*-amide backbone layer were fixed to the theoretical values during fitting. This is based on the assumption that the outer *n*-decyl side chains are more close to the equilibrium conformation at the topmost surface due to the so-called "free surface effect",[8] while the inner *n*-decyl side chains that are in direct contact to the Si substrate are kinetically trapped in an out-of-equilibrium state due to irreversible adsorption (or the pinning of the side chains).[9, 10] The free parameters used in the best-fits shown in Figure 6 (a) are the ρ_e and thickness of the inner *n*-decyl layer, and the interfacial roughness at the multiple interfaces, *i.e.*, silicon/inner *n*-decyl layer interface (σ_{Si}), inner *n*-decyl layer/*cis*-amide backbone interface (σ_1), *cis*-amide backbone/outer *n*-decyl layer interface (σ_2) and outer *n*-decyl layer/air interface (σ_3). It is necessary to mention that the use of models that composed of a single polymer layer or two polymer layers cannot adequately fit the XRR curves in Figure 6 (a) reasonably well. Rather, a three-polymer-layer model (Figure 8) with a lower electron density inner layer is essential to achieve the best-fits to the data with physically reasonable parameters. It should be noted that if the ρ_e and the thickness values of the *cis*-amide backbone layers and the outer *n*-decyl layers are set as free parameters, similar electron density profiles can be achieved during the optimization procedures to obtain best-fits to the data. Due to the presence of multiple parameters within the slab model and the limited sensitivity of XRR to the exact shape of the ρ_e perturbation at the interfaces, we do not claim that all parameters in Table 2 can be individually optimized. The overall electron density profile of polypeptoid monolayers near solid substrates can still be reliably determined with a good spatial resolution by fitting the reflected intensity profiles with reasonable parameters.

***In Situ* Grazing Incidence Wide-Angle X-Ray Diffraction (GIWAXD).** *In situ* grazing incidence wide-angle X-ray diffraction (GIWAXD) measurements for the *l*/*c*-PNDG thin films and adsorbed layers (sample size = 1 inch × 1 inch) were carried out at the Complex Materials Scattering (CMS/11-BM) beamline at the National Synchrotron Light Source II (NSLS-II), Brookhaven National Laboratory. Two-dimensional (2D) GIWAXD patterns were collected using a Photonic Science ImageStar CCD area detector (pixel size = 101.7 μm × 101.7 μm) or a Dectris Pilatus 800k area detector (pixel size = 172 μm × 172 μm). The detector distance was calibrated using a silver behenate standard sample. The incident angle of X-rays was set to 0.10° at λ = 0.0918 nm, which was just above

the critical angle of PNDG (0.09°) but below the critical angle of Si (0.13°), hence illuminating the entire film. *In situ* high temperature measurements were carried out under vacuum (~ 7×10^{-2} Torr) with a temperature-controlled sample stage interfaced with a Lakeshore 340 unit. To probe the phase transitions of *l*/*c*-PNDG films, the *in situ* experiments were carried out by first heating from room temperature up to 200 °C at 10 °C/min, successively cooling to 40 °C with a temperature interval of 10 °C, and then re-heating to 200 °C at 1 °C/min. At each temperature, the sample was equilibrated for 30 min before collecting GIWAXD. The exposure times were fixed to 30 sec for the thin films and 120 sec for the adsorbed layers. For the Pilatus detector, multiple 2D images per sample were collected with offset detector positions to avoid loss of information from the detector gaps. 2D GIWAXD 2D patterns were transformed into 1D profiles along the q_{xy}-direction (horizontal axis) and q_z-direction (vertical axis), with q_{xy} and q_z being the scattering vectors in the parallel and perpendicular directions to the film surface, respectively.

X-Ray Photoelectron Spectroscopy (XPS). X-ray photoelectron spectroscopy (XPS) measurements were performed by a PHI 5000 VersaProbe III system (Ulvac-PHI Inc., Chanhassen, MN, USA) equipped with a monochromatized Al *K*α X-ray source (1486.6 eV). All high-resolution spectra were referenced to the C 1s hydrocarbon peak at 284.8 eV. The take-off angles (*i.e.*, the angle between the sample surface normal and the central axis of the analyzer) of the photoelectrons were set at 45°, which corresponds to a sampling depth of approximately 4.5 nm. The survey spectra were obtained in the range of 0 - 1,100 eV at 1.0 eV energy steps and the high-resolution scans were operated at 0.125 eV energy steps.

Optical Microscopy (OM). Optical microscopy (OM) measurements were conducted by using reflective light under an Olympus BHT Microscope equipped with a differential interference contrast attachment for incident light after Nomarski (NIC Model). OM images were captured by a digital camera at room temperature.

Atomic Force Microscopy (**AFM).** Atomic force microscopy (AFM) (Agilent 5500 Keysight Technologies, USA) was used to study the surface morphologies of the *l*/*c*-PNDG thin films and adsorbed layers. A standard tapping mode was conducted in air using aluminum-coated silicon probes (RTESPA-300; Bruker, Inc., USA) with a frequency of ~ 300 kHz and a spring constant of 40 N/m.

The scan rate was 0.5 – 1.0 line/sec with scanning density of 512 lines per frame. The AFM imaging analysis was conducted using the Gwyddion software (version 2.47, http://gwyddion.net/).[11]

Contact Angle Measurements. The static contact angles of the linear or cyclic PNDG spin cast thin films and adsorbed layers were measured by using a VCA 2000 contact angle goniometer (VCA, Billerica, MA). The volume of each sessile liquid droplet was fixed to 2 μL. The static contact angles were collected 10s after the liquid droplet was dropped onto the sample surface, and we did not observe any change in the static contact angles for up to 2 min. A static contact angle (θ) of a film surface was determined by the three-phase contact line of the 2 μL liquid droplet. All the results were obtained by averaging data from at least 3 individual samples and 5 readings per sample at different locations. The static contact angles of the cyclic and linear PNDG films were found to be identical using water or ethylene glycol ($\theta = 103 \pm 1°$ for water and $\theta = 83 \pm 1°$ for ethylene glycol) (Figure S4).

Estimation of Surface Tension. The estimation of the surface tension was based on the two-component theory, *i.e.*, the polar component and the dispersion component. Based on the Young's equation (eq. S1), the Owens-Wendt-Kaelble equation (eq. S2), and the surface tensions of the test liquids (Table S1), the polar and dispersion components of the *l*/*c*-PNDGs could be calculated[3, 12]:

$$\gamma_s = \gamma_l \cos\theta + \gamma_{sl} \quad \text{(eq. S1)}$$

$$\gamma_{sl} = \gamma_l + \gamma_s - 2\left(\gamma_s^d \gamma_l^d\right)^{1/2} - 2\left(\gamma_s^p \gamma_l^p\right)^{1/2} \quad \text{(eq. S2)}$$

where γ_s and γ_l are the total surface tension of the solid and liquid, respectively. γ_{sl} is the interfacial energy between solid and liquid. θ is the static contact angle of the liquid. γ^d_s and γ^p_s are the dispersion and polar parts of the surface energy of the solid, respectively. γ^d_l and γ^p_l are the dispersion and polar parts of the surface energy of the liquid, respectively.

The surface tension (γ_{PNDG}) of both cyclic and linear PNDGs samples is estimated to be γ_{PNDG} = 16.2 mJ/m^2 with a dispersion part (γ^d_{PNDG}) of 14.1 mJ/m^2 and a polar part (γ^p_{PNDG}) of 2.1 mJ/m^2 by using the known surface tensions of the testing liquids (Table S2), experimentally determined static contact angle of the liquids on *c*/*l*-PNDG films (Figure S4) and eq. S1 and S2. Based on the surface tensions of the HF-treated Si substrate[13] and the native oxide Si substrate,[3, 14] the interfacial energy between the PNDG polymer and the HF-treated Si substrate is estimated to be $\gamma_{PNDG\text{-}Si}$ = 10.7 mJ/m^2 by using Eq. S2, while the interfacial energy between the polymer and the native oxide Si substrate is

estimated to be $\gamma_{PNDG\text{-}SiOxSi}$ = 14.9 mJ/m^2. Thus, the *l*/*c*-PNDGs have a stronger affinity with the HF-treated Si substrate comparing with the native oxide Si substrate.

Table S1. Molecular parameters of linear and cyclic PNDG polymers

Polymer	$[M]_0$:$[I]_0$ [a]	DP_n [b]	M_n (kg/mol) [c]	PDI [d]
l-PNDG	50:1	52	10.4	1.14
c-PNDG	50:1	50	10.2	1.11

[a.] Initial monomer-to-initiator ratio used in the polymerization; [b.] number-averaged degree of polymerization was determined by end-group analysis using ^{1}H NMR spectroscopy; [c.] M_n was calculated using the DP_n and molecular weight of the repeating unit; [d.] polydispersity index was determined by MALDI-TOF MS analysis of the respective PNDG polymers.

Scheme S1.

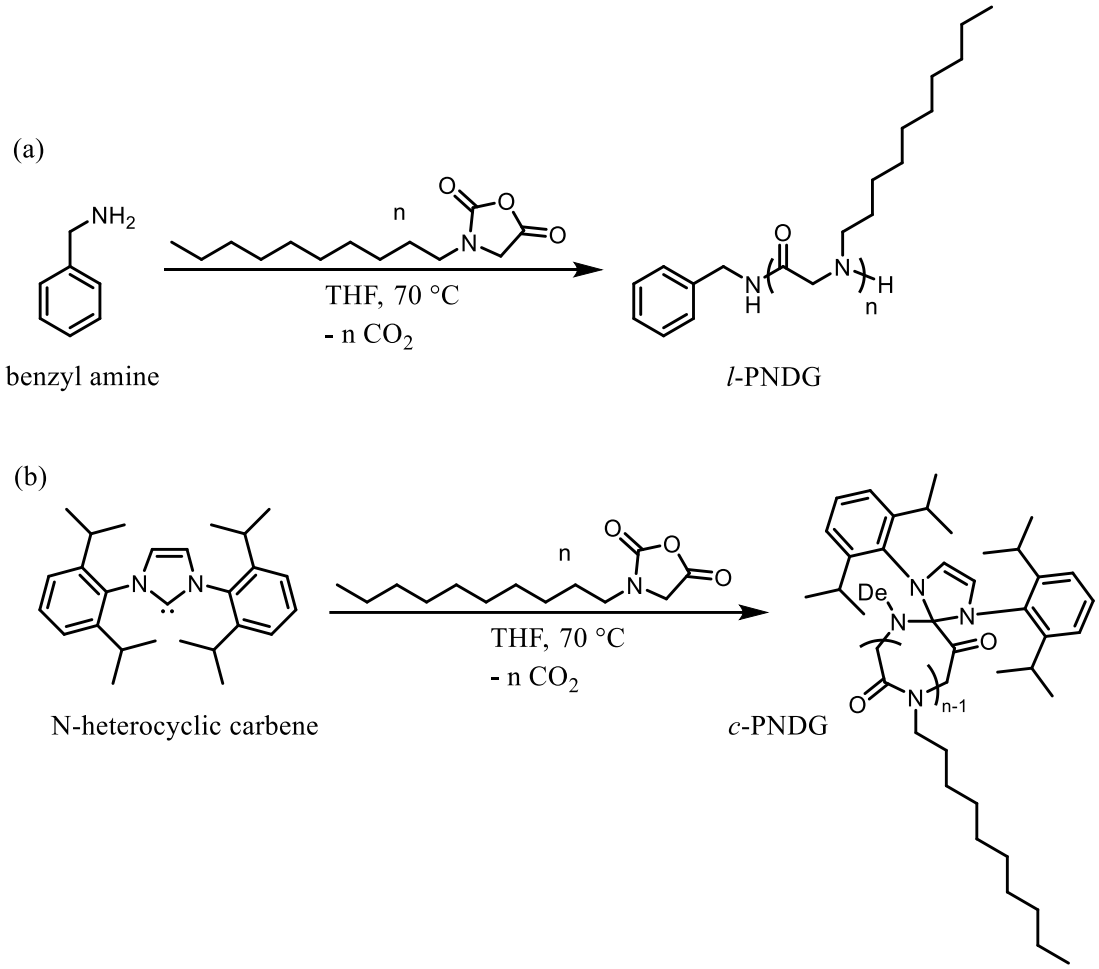

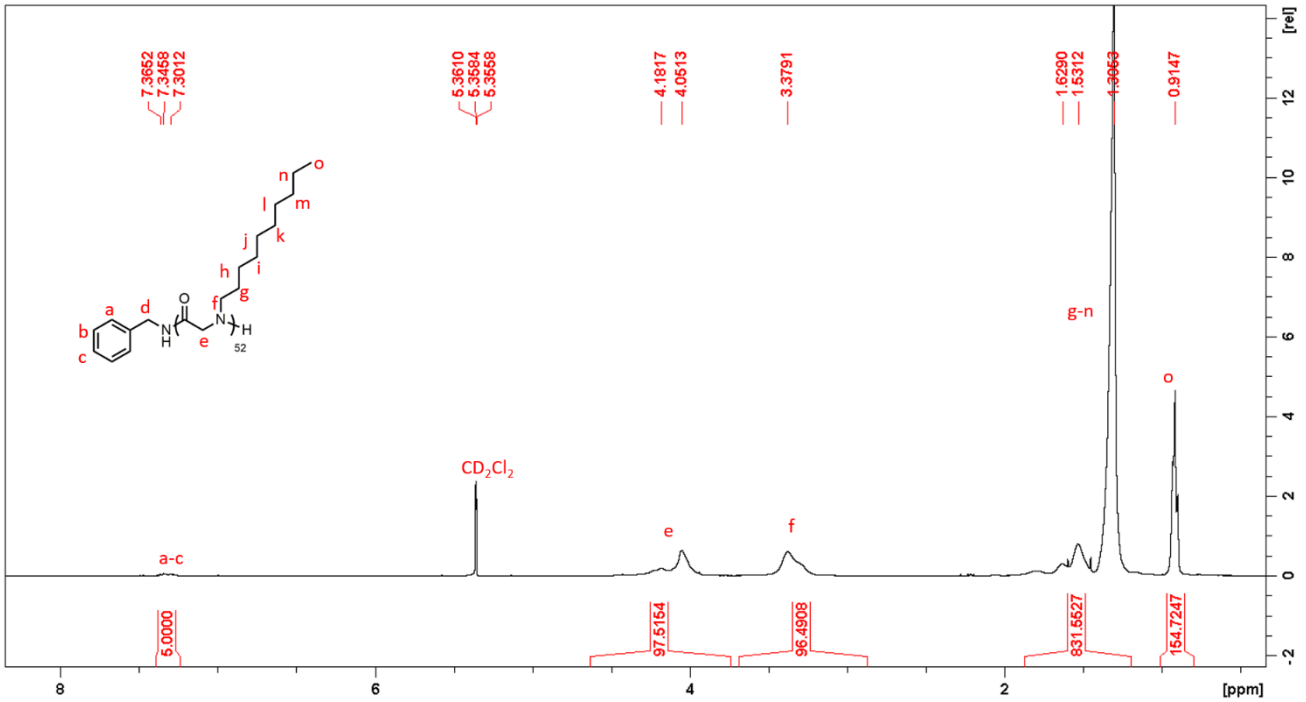

Figure S1. ^{1}H NMR spectrum of the *l*-PNDG polymer in CD_2Cl_2.

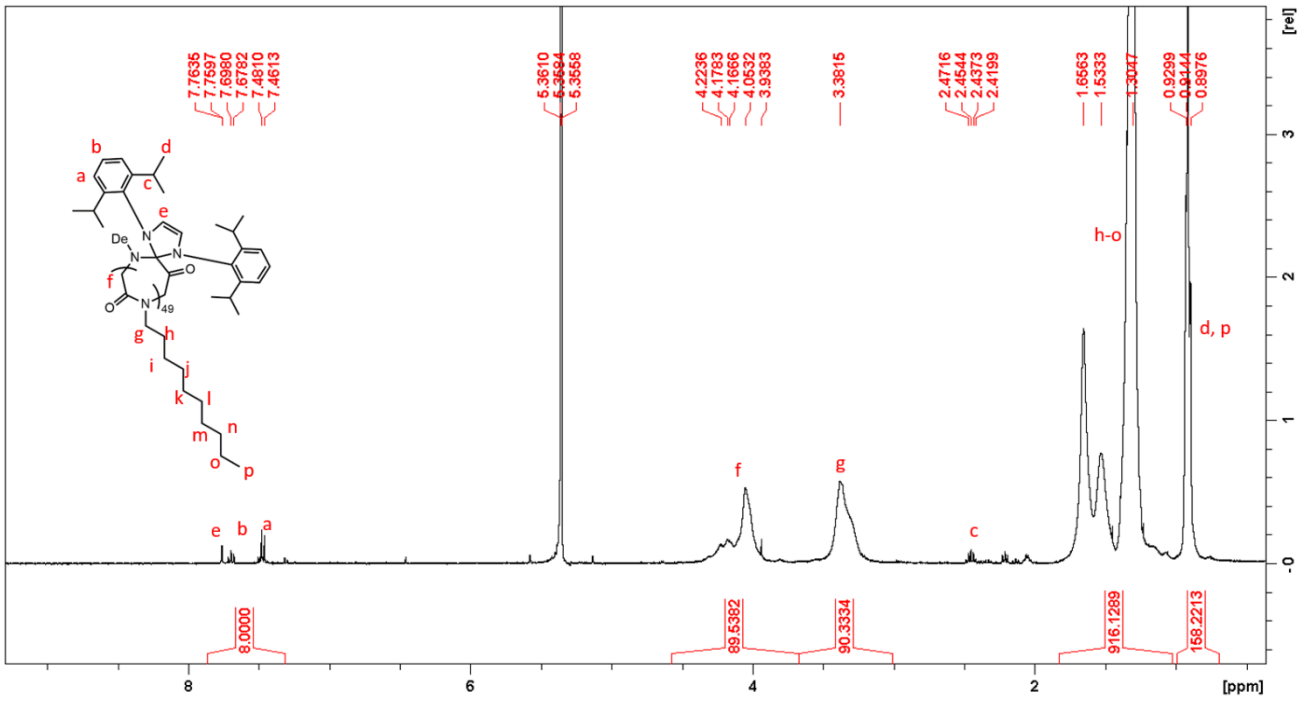

Figure S2. ^{1}H NMR spectrum of the *c*-PNDG polymer in CD_2Cl_2.

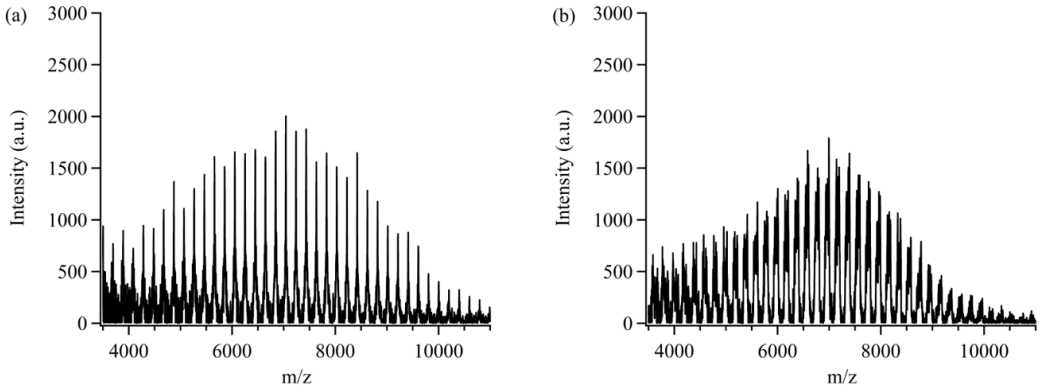

Figure S3. The MALDI-TOF MS spectra of (a) *l*-PNDG and (b) *c*-PNDG polymers.

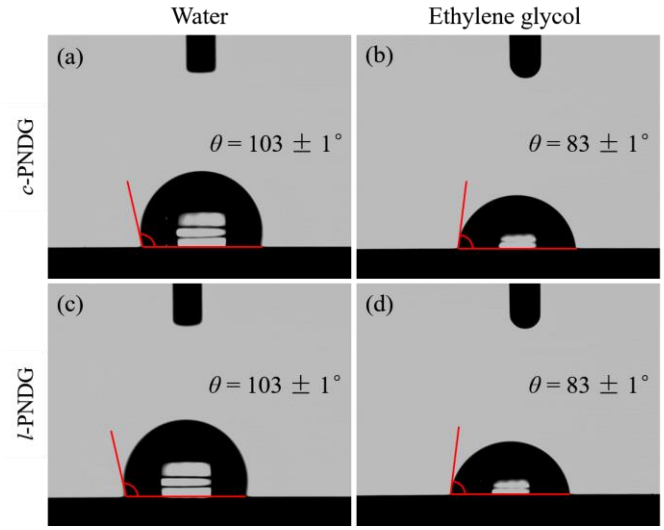

Figure S4. Static contact angles of (a, c) water and (b, d) ethylene glycol on top of the (a, b) *c*-PNDG and (c, d) *l*-PNDG films (48 nm in thickness). Note that these films were only pre-annealed at T = 200 ºC for 20 min, so that no dewetting was observed in any of these films. The static contact angles of the cyclic and linear PNDG films were identical (θ = 103 ± 1° for water and θ = 83 ± 1° for ethylene glycol). Thus, the surface tension of PNDG films are identical regardless of the chain architecture (*i.e.*, cyclic or linear).

Table S2. Surface tensions of the testing liquids at room temperature.[15]

Liquid	Surface Tension (γ_l, mJ/m^2)	Dispersion Component (γ_l^d, mJ/m^2)	Polar Component (γ_l^p, mJ/m^2)
Water	72.8	22.6	50.2
Ethylene Glycol	48.8	32.8	16.0

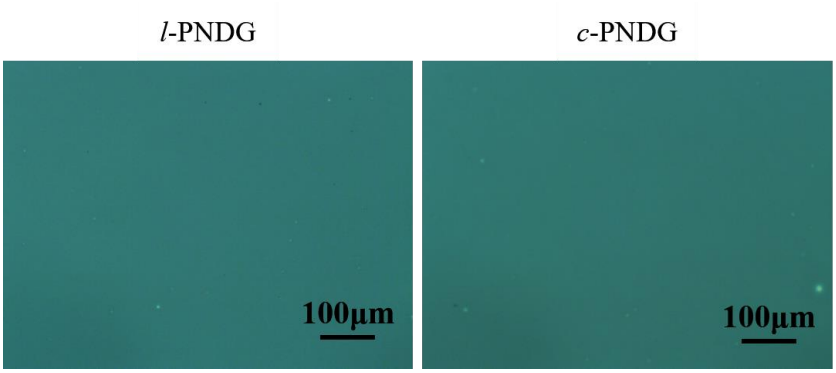

Figure S5. Representative optical microscopic (OM) images of the 111 nm-thick *l*-PNDG (left)and *c*-PNDG (right) as-cast films on Si substrates without any thermally annealing.

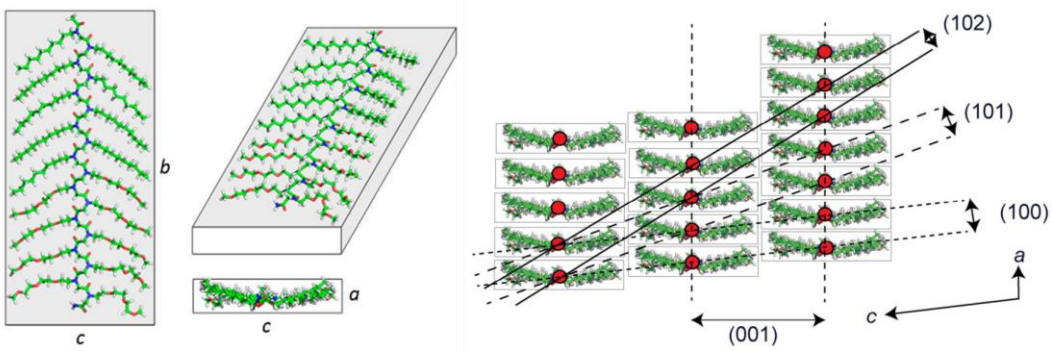

Figure S6. The unit cell dimensions and crystalline lattice of peptoid molecules with all *cis*-amide backbone conformation (Figure reproduced from the reference).[16] The all *cis*-amide backbone conformation, which is more compact and possess higher degree of order than the all *trans*-amide conformation, allows for more favorable intra- and inter-molecular interactions in intermolecular assemblies.[7, 16, 17] (Notes: Polypeptoids with long *n*-alkyl *N*-substituents ($4 \leq S \leq 14$, where S is the number of carbon atoms on the *n*-alkyl side chain) are highly crystallizable in both solid- and solution-states.[3, 7, 16, 17] In the crystalline state, peptoid molecules with N backbone repeating units and S number of carbon on the *n*-alkyl side chains adopt an energetically favorable all-*cis* backbone conformation, and the unit cell dimensions, namely a, b, and c, follow a universal relationship, in which a = 0.455 nm, b = (0.298N + 0.035) nm and c = (0.186S + 0.55) nm.[7] In addition, for longer crystallizable polypeptoids (*i.e.*, $N \geq 30$) obtained by polymerization methods, while the unit cell dimensions of a and c can be clearly identified from Bragg reflections under X-ray and consistent with the universal relationship, the b dimension often cannot be observed, possibly due to the presence of polydispersity and certain degree of backbone folding.)[3, 7]

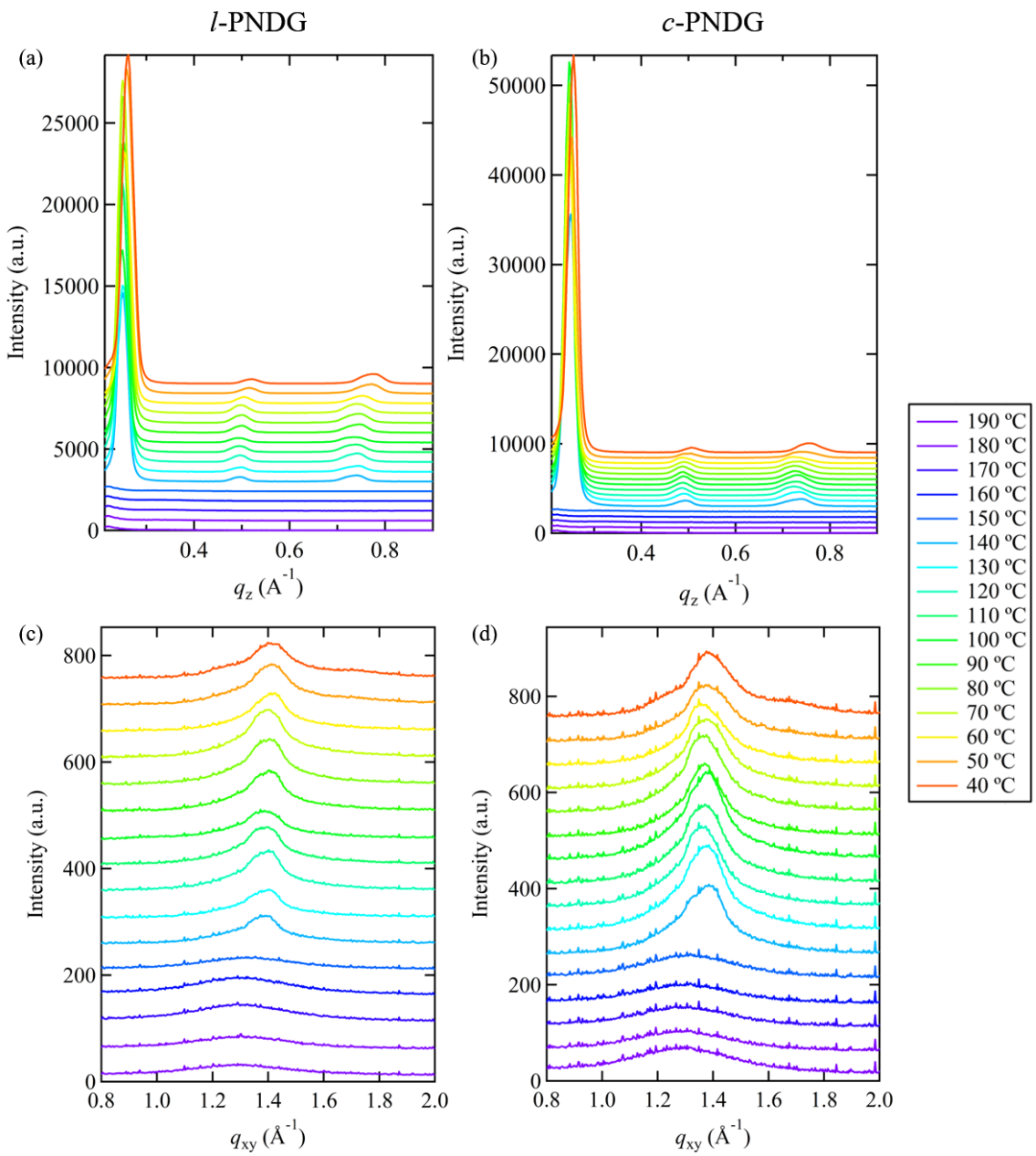

Figure S7. *In situ* one dimensional GIWAXD profiles of (a, c) *l*-PNDG and (b, d) *c*-PNDG along the q_z direction and q_{xy} direction through a cooling cycle. The films were first heated to 200 °C and hold at 200 °C for 10 min. GIWAXD measurements were then performed during a step cooling process from 200 °C to 40 °C with a temperature interval of 10 °C. At each given temperature, the films were equilibrated for approximately 30 min before data collection. A major structural transition at T = 140 °C due to the melt recrystallization of comb-shaped chains was observed for both *l*/*c*-PNDG films. A secondary transition at T = 50 °C is also discernible, which is attributed to the transition from a Sanidic liquid crystalline mesophase to a crystalline phase. The overall phase transition of *l*/*c*-PNDG films is consistent with previous findings on bulk polymers.[3, 16]

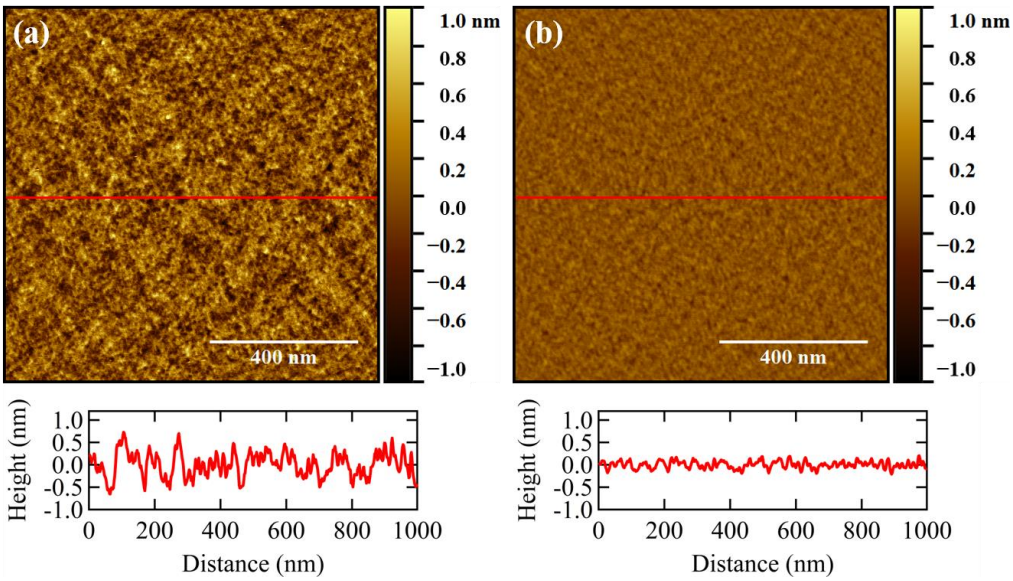

Figure S8. Representative AFM height image of (a) the dewetted region of the 48 nm-thick *l*-PNDG thin films and (b) the bare Si substrate. The height scale and scan size of both images are ± 1 nm and 1 μm × 1 μm, respectively. The corresponding height profiles along the red lines are shown below each AFM images. The surface RMS roughness of the dewetted region is estimated to be 0.27 nm, while the surface RMS roughness of bare Si substrate is c.a. 0.09 nm. The cross-sectional analysis of the AFM height images suggests that the dewetted region of the *l*-PNDG film is filled with a thin polymer layer on the Si substrate.

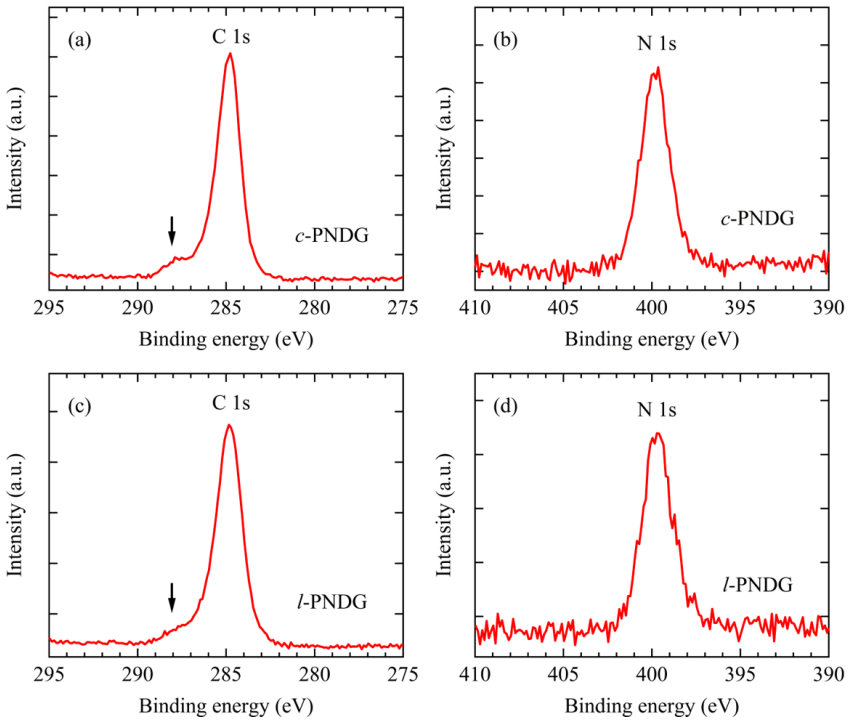

Figure S9. X-ray photoelectron spectroscopic (a, c) C 1s and (b, d) N 1s narrow scans of the *c*-PNDG (top row) and *l*-PNDG (bottom row) residual layers after solvent leaching with chloroform. The peaks corresponding to the amide (C(=O)N) groups of the polypeptoid backbone in (a) and (c) are indicated by the black arrows.

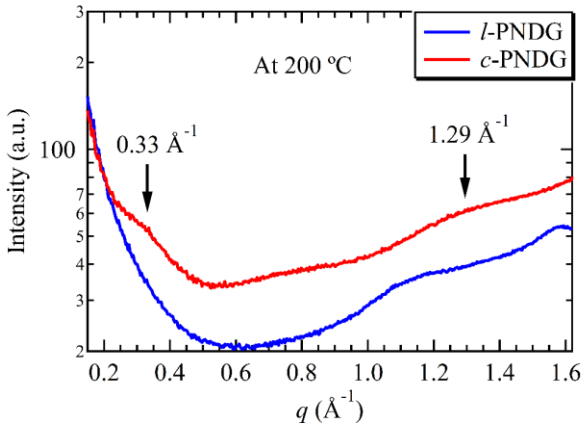

Figure S10. One-dimensional GIWAXD profiles (log $I(q)$ vs. q) of the *c*-PNDG (red lines) and *l*-PNDG (blue lines) adsorbed layers azimuthally integrated from 0° to 75° azimuthal angle with respect to the q_{xy} axis. Note that multiple GIWAXD images were collected with offset detector positions to cover gaps in the Pilatus detector.

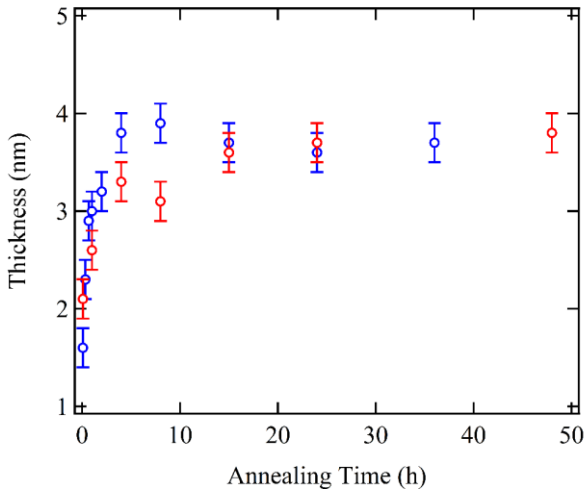

Figure S11. The plot of the thickness of the *l*-PNDG (blue circles) and *c*-PNDG (red circles) adsorbed layers on Si substrate versus annealing time at 200 °C under vacuum. The thicknesses were measured by a multi-wavelength spectroscopic ellipsometer and analyzed by using a Cauchy model.[5] Note: the adsorbed layer thicknesses obtained by ellipsometry were found to be about 0.5 nm larger than those obtained by XRR analysis (Table 2). Such discrepancy is possibly due to the limited accuracy of ellipsometry in measuring ultrathin polymer films.[18] Regardless, the adsorbed layer thickness was found to increase rapidly at the initial stage and arrives at a plateau regime (*a.k.a.* the quasi-equilibrium state of adsorption[19]) after 2-4 hours of annealing at 200 °C.

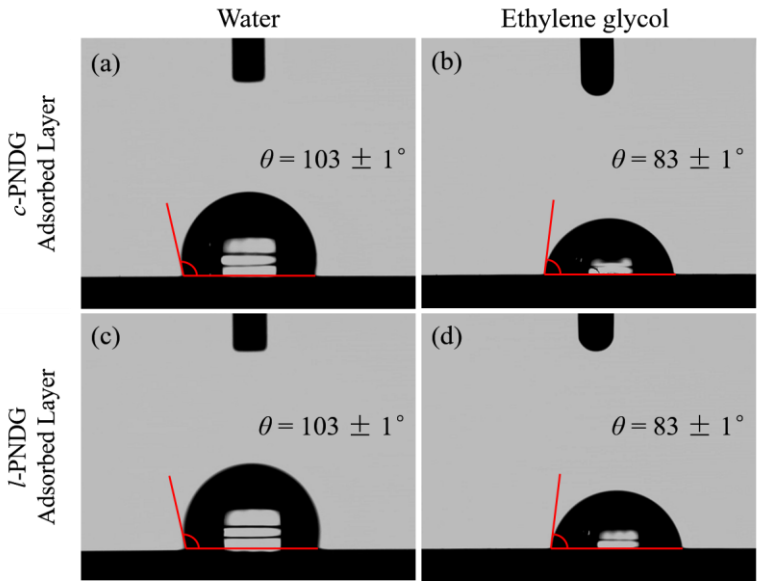

Figure S12. Static contact angles of (a, c) water and (b, d) ethylene glycol on top of the (a, b) *c*-PNDG and (c, d) *l*-PNDG adsorbed layers.

References

1. Guo, L.; Zhang, D. Cyclic poly(α-peptoid)s and their block copolymers from n-heterocyclic carbene-mediated ring-opening polymerizations of n-substituted n-carboxylanhydrides. *Journal of the American Chemical Society* **2009,** 131, (50), 18072-18074.

2. Lee, C.-U.; Smart, T. P.; Guo, L.; Epps, T. H.; Zhang, D. Synthesis and characterization of amphiphilic cyclic diblock copolypeptoids from n-heterocyclic carbene-mediated zwitterionic polymerization of n-substituted n-carboxyanhydride. *Macromolecules* **2011,** 44, (24), 9574-9585.

3. Lee, C.-U.; Li, A.; Ghale, K.; Zhang, D. Crystallization and melting behaviors of cyclic and linear polypeptoids with alkyl side chains. *Macromolecules* **2013,** 46, (20), 8213-8223.

4. Guiselin, O. Irreversible adsorption of a concentrated polymer solution. *Europhys. Lett.* **1992,** 17, (3), 225-230.

5. Synowicki, R. A. Spectroscopic ellipsometry characterization of indium tin oxide film microstructure and optical constants. *Thin Solid Films* **1998,** 313-314, 394-397.

6. Seeck, O. H.; Kaendler, I. D.; Tolan, M.; Shin, K.; Rafailovich, M. H.; Sokolov, J.; Kolb, R. Analysis of x-ray reflectivity data from low-contrast polymer bilayer systems using a fourier method. *Appl. Phys. Lett.* **2000,** 76, (19), 2713-2715.

7. Greer, D. R.; Stolberg, M. A.; Kundu, J.; Spencer, R. K.; Pascal, T.; Prendergast, D.; Balsara, N. P.; Zuckermann, R. N. Universal relationship between molecular structure and crystal structure in peptoid polymers and prevalence of the cis backbone conformation. *Journal of the American Chemical Society* **2018,** 140, (2), 827–833.

8. Priestley, R. D.; Ellison, C. J.; Broadbelt, L. J.; Torkelson, J. M. Structural relaxation of polymer glasses at surfaces, interfaces, and in between. *Science* **2005,** 309, (5733), 456-459.

9. Gin, P.; Jiang, N.; Liang, C.; Taniguchi, T.; Akgun, B.; Satija, S. K.; Endoh, M. K.; Koga, T. Revealed architectures of adsorbed polymer chains at solid-polymer melt interfaces. *Phys. Rev. Lett.* **2012,** 109, (26), 265501.

10. Panagopoulou, A.; Napolitano, S. Irreversible adsorption governs the equilibration of thin polymer films. *Physical Review Letters* **2017,** 119, (9), 097801.

11. Nečas, D.; Klapetek, P. Gwyddion: An open-source software for spm data analysis. *Cent. Eur. J. Phys.* **2012,** 10, (1), 181-188.

12. D. Y. Kwok, A. W. N. Contact angle measurement and contact angle interpretation. *Advanced in Colloid and Interface Science* **1999,** 81, 167-249.

13. Wang, Y.; Rafailovich, M.; Sokolov, J.; Gersappe, D.; Araki, T.; Zou, Y.; Kilcoyne, A. D. L.; Ade, H.; Marom, G.; Lustiger, A. Substrate effect on the melting temperature of thin polyethylene films. *Phys. Rev. Lett.* **2006,** 96, (2), 028303.

14. Kawai, A.; Kawakami, J.; Sasazaki, H. Surface energy change of si(100) wafer by exposing to air. *Journal of Photopolymer Science and Technology* **2008,** 21, (6), 739-740.

15. Mittal, K. L., *Contact angle, wettability and adhesion, volume 4*. CRC Press: 2006.

16. Greer, D. R.; Stolberg, M. A.; Xuan, S.; Jiang, X.; Balsara, N. P.; Zuckermann, R. N. Liquid-crystalline phase behavior in polypeptoid diblock copolymers. *Macromolecules* **2018,** 51, (23), 9519-9525.

17. Edison, J. R.; Spencer, R. K.; Butterfoss, G. L.; Hudson, B. C.; Hochbaum, A. I.; Paravastu, A. K.; Zuckermann, R. N.; Whitelam, S. Conformations of peptoids in nanosheets result from the interplay of backbone energetics and intermolecular interactions. *Proceedings of the National Academy of Sciences* **2018,** 115, (22), 5647-5651.

18. Fujiwara, H., *Spectroscopic ellipsometry: Principles and applications*. John Wiley & Sons: 2007.

19. Jiang, N.; Shang, J.; Di, X.; Endoh, M. K.; Koga, T. Formation mechanism of high-density, flattened polymer nanolayers adsorbed on planar solids. *Macromolecules* **2014,** 47, (8), 2682-2689.